Modelling the bidirectional reflectance distribution function (BRDF) of seawater polluted by an oil film

Zbigniew Otremba

Gdynia Maritime University, Morska 81-87, PL 81 225 Gdynia, Poland
zot@am.gdynia.pl

Jacek Piskozub

Institute of Oceanology PAS, Powstancow Warszawy 55, PL 81 712 Sopot, Poland
piskozub@iopan.gda.pl

Abstract: The Bi-directional Reflectance Distribution Function (BRDF) of both clean seawaters and those polluted with oil film was determined using the Monte Carlo radiative transfer technique in which the spectrum of complex refractive index of *Romashkino* crude oil and the optical properties of case II water for chosen wavelengths was considered. The BRDF values were recorded for 1836 solid angular sectors of throughout the upper hemisphere. The visibility of areas polluted with oil observed from various directions and for various wavelengths is discussed.

OCIS codes: (330.1800) Contrast sensitivity; (010.4450) Ocean optics; (310.6860) Thin film, optical properties; (999.9999) Modelling of BRDF; (999.9999) Marine pollution monitoring

References and links

1. Z. Otremba and J. Piskozub, "Modelling of the optical contrast of an oil film on a sea surface," Opt. Express **9,** 411-416 (2001), http://www.opticsexpress.org/abstract.cfm?URI=OPEX-9-8-411.
2. Gao, F., C. B. Schaaf, A. H. Strahler, Y. Jin, and X. Li, 2003, "Detecting vegetation structure using a kernel-based BRDF model," Remote Sens. Environ. **86**, 198-205.
3. Mobley C. D., H.Zsang, K. J. Voss, 2003, "Effects of optically shallow bottoms on upwelling radiances: Bidirectional reflectance distribution function effects," Limnol. Oceanogr. **48,** 337-345.
4. Z. Otremba, "Relationship between the quantities which describe reflective features of both land and ocean areas," Proc. II International Conference on Current Problems in Optics of Natural Waters, September 8-12, 2003, St. Petersburg, Russia, Petersburg (Russia) 2003, http://am.gdynia.pl/~zot/ONW2003-Otremba.pdf
5. Schaaf, C. B., F. Gao, A. H. Strahler, W. Lucht, X. Li, T. Tsang, N. C. Strugnell, X. Zhang, Y. Jin, J.-P. Muller, P. Lewis, M. Barnsley, P. Hobson, M. Disney, G. Roberts, M. Dunderdale, C. Doll, R. d'Entremont, B. Hu, S. Liang, and J. L. Privette, "First Operational BRDF, Albedo and Nadir Reflectance Products from MODIS," Remote Sens. Environ. **83,** 135-148 (2002).
6. S. Sagan, Institute of Oceanology, Powstancow Warszawy 54, 81-712 Sopot, Poland (personal communication, 2002).
7. T. Petzold, "Volume scattering functions for selected ocean waters," In: *Light in the sea*, J. E. Tyler (Ed) Dowden, Hutchinson & Ross, Stroudsburg, Pa, 152-174 (1977)
8. A. Vasicek, *Optics of thin film* (North Holland, Amsterdam, 1960).

1. Introduction

The studies focused on the visibility of oil slicks for light detectors positioned in the plane of solar light of incidence were described in our previous paper [1]. However, recent improvements in the Monte Carlo code used by us made it possible to calculate relatively precisely the radiation field for the whole hemisphere. The Bi-directional Reflectance Distribution Function (BRDF) - as a function of incidence zenith angle, incidence azimuth angle, reflection zenith angle and reflection nadir angle, as well as wavelength - is widely implemented in land remote sensing, especially for vegetation quality assessment [2]. However, it has only been occasionally applied in marine optics to date. One of the few

#4017 - $15.00 US Received 11 March 2004; revised 29 March 2004; accepted 2 April 2004

recent examples is in the paper by Mobley *et al*. [3] in which BRDF was used to characterise optically shallow bottoms. However, the more frequent utilisation of sea/ocean BRDF should be anticipated as it provides much more information than the 'traditional' reflectances used in ocean optics, i.e., radiance reflectance, remote sensing reflectance, irradiance reflectance, *etc*. [4]. Additionally, the continuous refinement of satellite techniques [5] makes the modelling of BRDF a useful tool in remote sensing studies.

A rigorous Bi-directional Reflectance Distribution Function r definition has the following differential form (1):

$$r(\theta_i, \varphi_i, \theta_r, \varphi_r, \lambda) = \frac{dL_r(\theta_r, \varphi_r, \lambda)}{L_i(\theta_i, \varphi_i, \lambda) \sin\theta_i \cos\theta_i \, d\theta_i \, d\varphi_i \, d\lambda} \tag{1}$$

where: θ_i and φ_i are angular coordinates for incident radiance and θ_r and φ_r – coordinates for radiance leaving the sea surface (often called as reflected radiance). The denominator expresses the infinitesimal contribution to incident irradiance which is generated by the incident *radiance* L_i from direction θ_i, φ_i. The numerical counterpart, related to a defined wavelength, is a simple ratio of reflected radiance to incident irradiance (2).

$$r(\theta_i, \varphi_i, \theta_r, \varphi_r, \lambda) = \frac{L_r(\theta_r, \varphi_r)}{E_i(\theta_i, \varphi_i)} \tag{2}$$

where: E_i expresses a number of virtual incident photons multiplied by the cosine of the angle of incidence θ_i, whereas L_r is a number of photons captured in a defined solid angle multiplied by the cosine of the angle of reflection θ_r and divided by value of that solid angle.

2. Model of the investigated environment

Both clean sea areas and those polluted with oil film are studied in this paper. In both cases, the model of the sea body is identical. Namely, the optical properties of the water are represented by absorption coefficient *a*, scattering coefficient *b* and by volume scattering function β. Typical values of the absorption coefficient and the scattering coefficient for turbid coastal case II sea water appropriate for the Gulf of Gdansk in the southern Baltic Sea (Tab. 1) [6] were used, whereas volume scattering function β characteristic for turbid water after Petzold [7] was applied.

Table 1. Optical parameters of natural seawater at various wavelengths.

Optical parameter	at 420 nm	at 450 nm	at 500 nm	at 550 nm	at 600 nm	at 650 nm	at 700 nm
Light absorption coefficient a (m^{-1})	0.7	0.35	0.3	0.27	0.4	0.5	0.8
Light scattering coefficient b (m^{-1})	0.7	0.6	0.5	0.5	0.45	0.45	0.55

Oil film floating on water surface modifies its optical features, which is manifested in the Monte Carlo simulation by replacing traditional Fresnel rules with the four following angular functions (1): two transmittances - different for upward ($T_\uparrow$) and downward light ($T_\downarrow$); two reflectances - also for upward ($R_\uparrow$) and downward light ($R_\downarrow$). The transmittances and reflectances were derived using traditional solutions appropriate for thin films [8]. The optical properties of *Romashkino* crude oil (one-day artificially aged as oil film on sea surface) were used during the derivations (Fig. 1). The optical characteristics of most aged crude oils are similar to those applied.

#4017 - $15.00 US Received 11 March 2004; revised 29 March 2004; accepted 2 April 2004

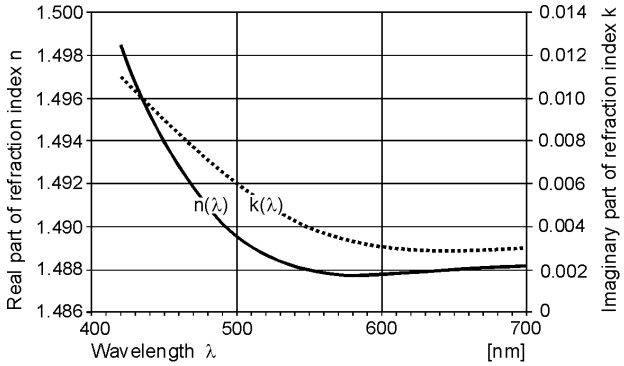

Fig. 1. Spectra of components of complex refraction index of *Romashkino* crude oil.

The transmittances and reflectances at wavelengths of 420, 450, 500, 550, 600, 650 and 700 nm were calculated. Distinct differences between the shapes of angular dependencies of reflectances and transmittances are visible mainly in the wavelength range from 420 nm to 550 nm. Angular dependencies of transmittances and reflectances for two wavelengths (420 and 550 nm) are presented in Fig. 2.

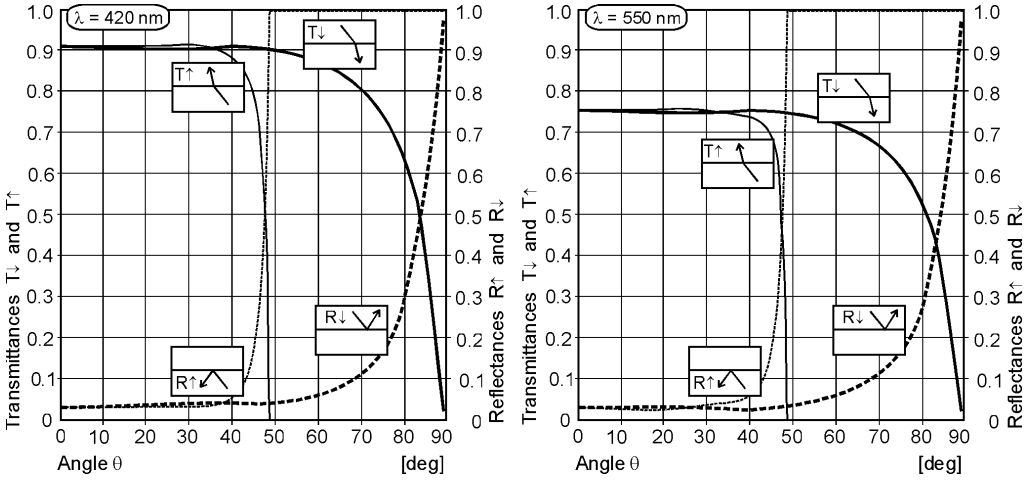

Fig. 2. Exemplary angular dependencies of transmittances and reflectances for water surface covered by an oil film of 1μm thickness, for two wavelengths: 420 nm (the left chart) and 550 nm (the right chart). Solid lines presents transmittances, broken lines – reflectances. Thick lines represent downward light, thin ones – upward light.

3. Monte Carlo model settings

Every Monte Carlo simulation was carried out using 1 billion incident photons. The upper hemisphere was covered by 1836 virtual receivers (of various solid angle values), 1296 of which captured aquatic-living photons in sectors of a size of 0.004363323130 sr; 252 – 0.001745329252 sr; 144 – 0.000872664626 sr; 144 – the narrowest and closest to the zenith sectors of a size 0.000436332313 sr. Thus, it was possible to obtain values of BRDF for a given angle of solar light incidence for all 1836 directions as the output data.

4. Results

The clearest way to graphically represent BRDF is by presenting the plots in cylindrical coordinates. The left part of Fig. 1 shows traditional placement of the nadir/zenith and azimuth angles in space; the right one explains the same in cylindrical coordinates suitable for

#4017 - $15.00 US Received 11 March 2004; revised 29 March 2004; accepted 2 April 2004

a graphic showing the BRDF. Exemplary (for two wavelengths) results of simulations - separately for a clean sea area and for that polluted by oil film - are presented in Fig. 4.

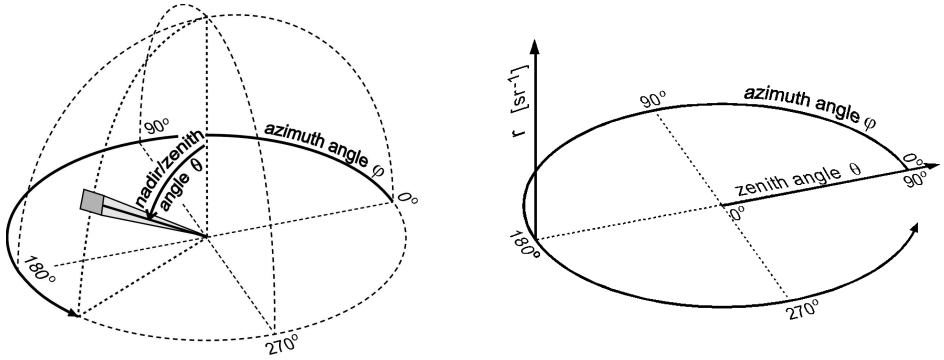

Fig. 3. Explanation of coordinates for presenting the Bidirectional Reflectance Distribution Function (BRDF) r: transformation from hemisphere coordinates (left plot) to cylindrical coordinates (right plot).

BRDF appears azimuthally symmetric only for vertical solar illumination. In other cases, the graphs become azimuthally asymmetric with the increase of the solar incident light zenith angle. The graphs in Fig. 4 relate to an angle of incidence of 40^o. Here the shape of the BRDF observed is characteristically bimodal, i.e., two local maximums occur. The first maximum appears near the direction of light incidence (backscattering light), the second is near the direction of specular reflection. There is displacement between the second maximum and specular reflection direction. Other tests reveal the variability of this displacement depending on the direction of solar incident radiance.

The shape of BRDFs appears to be similar for clean sea areas and those polluted by thin oil film. To display the difference between the BRDF for clean and polluted areas contrast *C* (3), that represents the visibility of oil film at defined wavelength, was calculated:

$$C = \frac{r_o - r_c}{r_c} \tag{3}$$

where: r_o indicates BRDF for a polluted sea area, r_c – for a clean one.

#4017 - $15.00 US Received 11 March 2004; revised 29 March 2004; accepted 2 April 2004

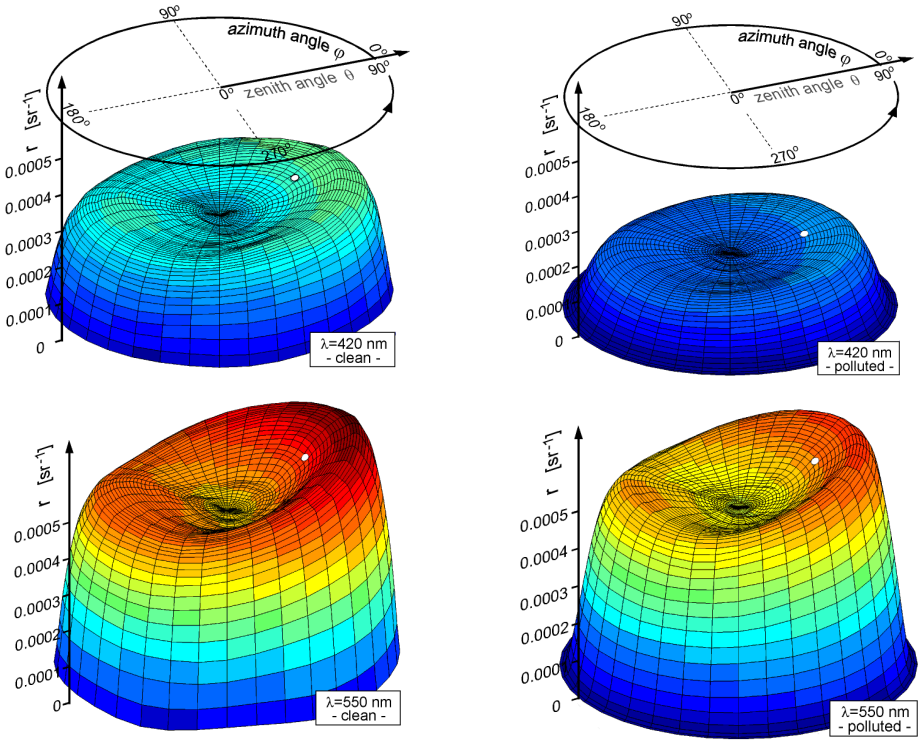

Fig. 4. Bidirectional Reflectance Distribution Function (BRDF) r for a clean sea-surface and for one polluted with oil film (the graphs on the left represent the clean surface, those on the right – the polluted one) and for two wavelength (420 nm – upper graphs; 550 nm – lower graphs). The white dots indicate the direction of specular reflection.

The shape of the contrast is circularly symmetric around the zenith direction (unlike BRDF), with no visible dependence on the direction of solar light incidence (Fig. 5). There is a plateau of contrast values when the zenith angle is less than 60°. For greater values, it starts to increase rapidly towards the value of minus one when the zenith angle approaches 90°. Additional tests performed revealed that the plateau moves to high values by about 10% when the angle of solar light incidence increases from 0 to 60°.

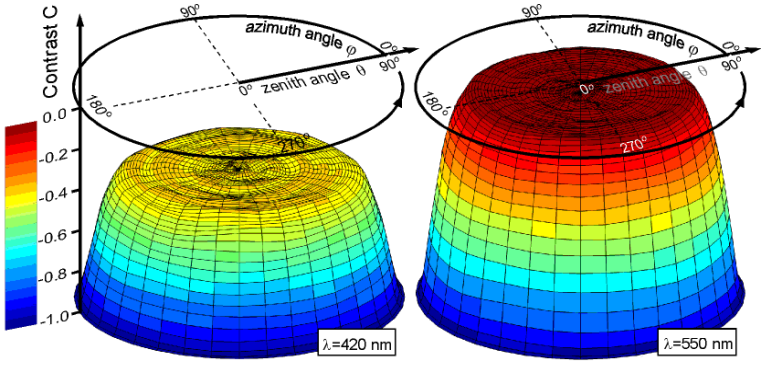

Fig. 5. Contrast C calculated for sea areas polluted by oil film for two wavelengths: 420 nm (left chart) and 550 nm (right chart), observed at 1836 various angles throughout the hemisphere.

#4017 - $15.00 US Received 11 March 2004; revised 29 March 2004; accepted 2 April 2004

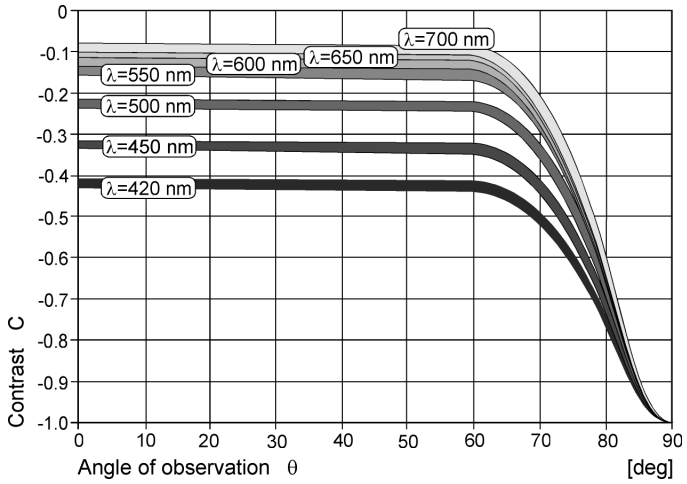

Fig. 6. Contrast of seawater polluted by an oil film vs. angle of observation for various wavelengths. The Avery plot consists of 1836 points (covering the whole hemisphere) obtained from Monte Carlo simulations.

It is characteristic that the contrast of areas polluted with oil film to clear sea areas strongly depends on wavelength. To display this, the angular dependencies of contrast for various wavelengths were presented in the same coordinates (Fig. 6). Greater values of contrast are observed at short wavelengths than at long wavelengths. Contrast decreases rapidly between 420 and 550 nm. Afterwards, the rate of decrease becomes smaller. It is worth mentioning that results obtained can be distorted by specular reflections from surface wave slopes. Therefore, the direction of observation should be chosen far from the direction where there is a high probability of sun glitter occurrence.

5. Conclusions

The values of BRDF for the sea surface are always smaller for the short-wave segment of the light spectrum than for middle and long-wave ones. The angular distribution of BRDF strongly depends on the direction of solar light incidence and is axially asymmetric around the zenith direction - excluding the case of vertical solar incident radiance. On the other hand, the distribution of the contrast of polluted area vs. observation direction is always axially symmetric. Additionally, the 3-D charts of contrast distribution have a plateau up to zenith angle of 60^{o}; at a larger zenith angle the contrast increases rapidly and approaches minus one at 90^{o}. Within the plateau, the absolute value of contrast is several times greater at the short-wave end of the light spectrum than for wavelengths from the middle and long end of the spectrum.

Acknowledgments

This paper was supported by a grant from the Gdynia Maritime University.

#4017 - $15.00 US Received 11 March 2004; revised 29 March 2004; accepted 2 April 2004